ACS chemical biology

Articles

pubs.acs.org/acschemicalbiology

Anticancer/Antiviral Agent Akt Inhibitor-IV Massively Accumulates in Mitochondria and Potently Disrupts Cellular Bioenergetics

J. Matthew Meinig and Blake R. Peterson*

Department of Medicinal Chemistry, The University of Kansas, Lawrence, Kansas 66045, United States

Supporting Information

ABSTRACT: Inhibitors of the PI3-kinase/Akt (protein kinase B) pathway are under investigation as anticancer and antiviral agents. Akt inhibitor-IV (ChemBridge 5233705, CAS 681281-88-9, AKTIV), a small molecule reported to inhibit this pathway, exhibits potent anticancer and broad-spectrum antiviral activity. However, depending on concentration, this cationic benzimidazole derivative exhibits paradoxical positive or negative effects on the phosphorylation of Akt that are not well understood. To elucidate its mechanism of action, we investigated its spectroscopic properties. This compound proved to be sufficiently fluorescent (excitation λ_{max} = 388 nm, emission λ_{max} = 460 nm) to enable examination of its uptake and distribution in living mammalian cells. Despite a low quantum yield of 0.0016, imaging of HeLa cells treated with AKTIV (1 μM, 5 min) by confocal laser scanning microscopy, with excitation at 405 nm, revealed extensive accumulation in mitochondria. Treatment of Jurkat lymphocytes with 1 μM AKTIV for 15 min caused accumulation to over 250 μM in these organelles, whereas treatment with 5 μM AKTIV yielded concentrations of over 1 mM in mitochondria, as analyzed by flow cytometry. This massive loading resulted in swelling of these organelles, followed by their apparent disintegration. These effects were associated with profound disruption of cellular bioenergetics including mitochondrial depolarization, diminished mitochondrial respiration, and release of reactive oxygen species. Because mitochondria play key roles in both cancer proliferation and viral replication, we conclude that the anticancer and antiviral activities of AKTIV predominantly result from its direct and immediate effects on the structure and function of mitochondria.

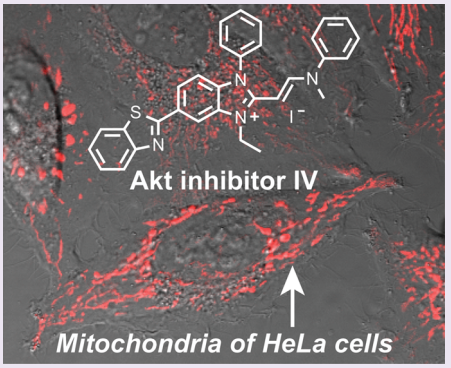

Akt inhibitor-IV (ChemBridge 5233705, CAS 681281-88-9, AKTIV, Figure 1), a cationic benzimidazole derivative,

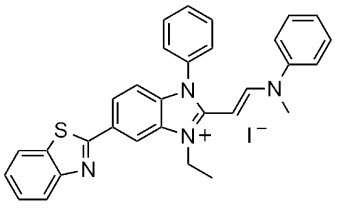

Akt inhibitor-IV (AKTIV)

Figure 1. Structure of Akt inhibitor-IV (AKTIV).

exhibits a wide range of biological activities. This small molecule was first identified in a chemical genetic screen as an inhibitor of nuclear export of the FOXO1a protein.[1] In U2OS cancer cells, low concentrations of AKTIV (IC_{50} = 0.625 μM) blocked nuclear export of this protein with concomitant inhibitory effects on cellular proliferation (IC_{50} < 1.25 μM).[1] At a higher concentration of 10 μM, phosphorylation of the serine-threonine kinase Akt (protein kinase B) on residues Ser473 and Thr308 was suppressed. Because phosphorylation of FOXO1a by Akt promotes nuclear export, AKTIV was initially proposed to block nuclear export of this protein by inhibiting a kinase in the PI3-kinase (PI3K)/Akt pathway.[1] Other studies of AKTIV confirmed its potent cytotoxic activity (typical IC_{50} values <2 μM) against a wide range of cancer and other cell lines.[2−7] Although some inhibitors of the PI3K/Akt pathway show promise as anticancer agents,[8,9] more recent studies[10] of AKTIV concluded that this compound does not directly block the activity of any known kinases within this signaling cascade. Moreover, AKTIV paradoxically increases phosphorylation of Akt when added to BHK-21 cells at 1−2 μM.[10] High concentrations (10 μM) of this small molecule also activate the unfolded protein response (UPR) and trigger cellular blebbing and apoptosis in HEK293T cells.[11]

In addition to its major effects on cellular proliferation, AKTIV exhibits broad-spectrum antiviral activity. Viruses inhibited by this compound include vesicular stomatitis virus (VSV), respiratory syncytial virus, vaccinia virus in infected BHK-21 cells,[10] and parainfluenzavirus-5 (PIV5) in infected HeLa cells.[12−14] However, the mechanistic basis for this activity is not well understood, the importance of the PI3K/Akt pathway in viral replication is controversial, and AKTIV has

Received: October 21, 2014
Accepted: November 21, 2014
Published: November 21, 2014

   dx.doi.org/10.1021/cb500856c | ACS Chem. Biol. 2015, 10, 570−576

been reported to block the replication of negative-strand RNA viruses through a Akt-independent mechanism.[10]

To probe the structural features associated with this highly biologically active scaffold, we previously reported the synthesis of AKTIV and a collection of analogues.[13] We demonstrated that this compound and some analogues exhibit selective anticancer activity against human HeLa carcinoma cells when compared with normal human bronchial/tracheal epithelial (NBHE) cells. We further confirmed its antiviral effects against recombinant parainfluenzavirus-5 in HeLa cells. Although the photophysical properties of these compounds have not been previously characterized, during our prior studies of analogues of AKTIV, we noticed that some of these compounds were qualitatively fluorescent in solution, and this observation led us to hypothesize that the intrinsic fluorescence of Akt inhibitor-IV, similar to other fluorescent molecular probes,[15,16] might reveal aspects of its biological mechanism of action. Using this approach, we found that AKTIV rapidly accumulates to high levels in mitochondria of treated mammalian cells and profoundly affects the morphology of these organelles. Treatment of cancer cell lines with AKTIV rapidly triggers extensive mitochondrial dysfunction, and this new understanding of its mechanism of action explains many of the diverse biological activities of this potent small molecule.

RESULTS AND DISCUSSION

During our prior studies of AKTIV,[13] we observed that dilute solutions of this compound are qualitatively fluorescent when irradiated with ultraviolet light. To examine the photophysical properties of this compound in detail, we obtained absorbance, fluorescence excitation, and fluorescence emission spectra in aqueous buffer (PBS, pH 7.4) and ethanol. As shown in Figure 2, the spectral properties of AKTIV in both of these solvents

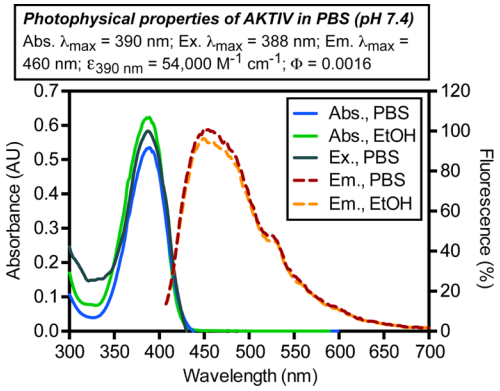

Figure 2. Photophysical properties of AKTIV. The absorbance (Abs.) spectrum, excitation (Ex.) spectrum, and fluorescence emission (Em.) spectrum were obtained in PBS (pH 7.4) and ethanol. Values for the extinction coefficient (ε), and quantum yield (Φ) in PBS are listed above.

were very similar, indicating that unlike some common fluorophores, such as dansyl, NBD, and certain coumarins,[17] its fluorescence properties are not highly sensitive to environmental conditions. In these solvents, AKTIV was found to strongly absorb in the UV–violet region (absorbance $\lambda_{max,\ PBS}$ = 390 nm), with a relatively high extinction coefficient ($\varepsilon_{390\ nm}$) in PBS of 54 000 M^{-1} cm^{-1}. Upon excitation with UV ($\lambda_{max,\ ex.}$ = 388 nm, Figure 2), AKTIV emitted blue fluorescence with λ_{max} = 460 nm (Figure 2). However, the quantum yield (Φ) of AKTIV was only 0.0016, as determined by comparison with the integrated emission of the coumarin-derived fluorophore Pacific Blue (Φ = 0.75, $\lambda_{max,abs}$ = 405 nm, $\lambda_{max,em}$ = 450 nm).[18,19] When the brightness of these two fluorophores was compared, defined as the product of the quantum yield and extinction coefficient, AKTIV was 260-fold less bright than Pacific Blue (ε_{405nm} = 30 000 M^{-1} cm^{-1}).[19] However, the relatively close match of the maximal excitation wavelength (388 nm) of AKTIV to the 405 nm laser line of many confocal laser scanning microscopes and flow cytometers led us to conclude that the intrinsic fluorescence of this compound might enable imaging and analysis of its subcellular distribution in living mammalian cells.

To investigate the utility of AKTIV as a fluorescent probe, HeLa cervical carcinoma cells were briefly treated (5 min) with a low concentration (1 μM) of this compound. Imaging by confocal laser scanning microscopy, with excitation at 405 nm, revealed fluorescence in defined subcellular structures of treated cells (Figure 3). These structures exhibited a tubular morphology and were identified as mitochondria by costaining with the spectrally orthogonal probe MitoTracker Deep Red-FM. To examine if autofluorescence of NADH[20] in these organelles contributed to this signal, control experiments in the absence of AKTIV were used to verify that the fluorescence

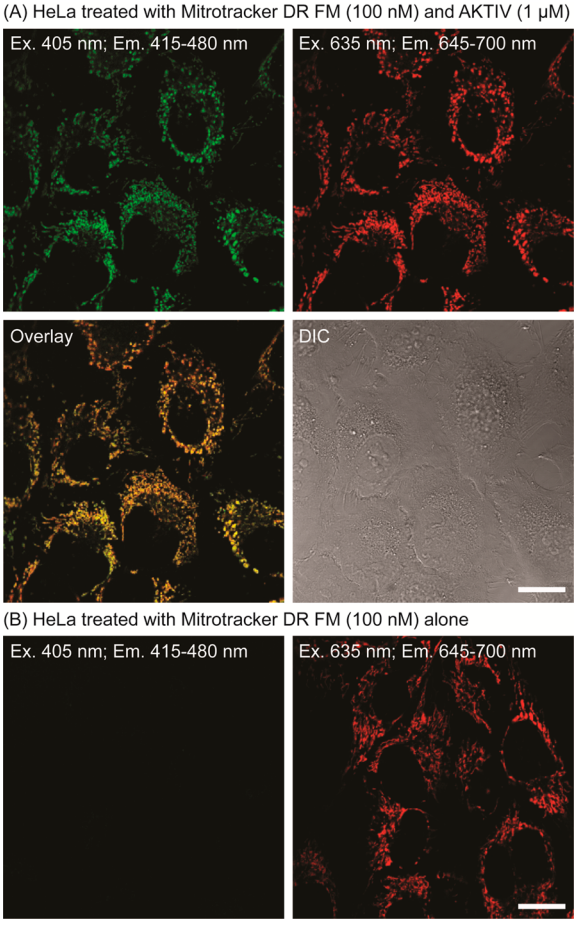

Figure 3. Confocal laser scanning and DIC micrographs of living HeLa cells. Cells in panel A were treated with MitoTracker Deep Red FM (100 nM) and AKTIV (1 μM) for 5 min. Cells in panel B were treated with MitoTracker Deep Red FM (100 nM, 5 min) alone to confirm the absence of autofluorescence under these conditions. The instrument settings and imaging parameters are identical in panels A and B. Scale bar = 20 μm.

dx.doi.org/10.1021/cb500856c | ACS Chem. Biol. 2015, 10, 570–576

observed in mitochondria upon excitation at 405 nm was exclusively derived from this compound (Figure 3). Because of its low quantum yield, the visualization of AKTIV in mitochondria of treated HeLa cells suggested that this compound accumulates to high levels in these organelles.

As shown in Figure 4, AKTIV shows structural similarities to MitoTracker Deep Red-FM,[21] JC-1,[22] rhodamine 123,[23] MKT-

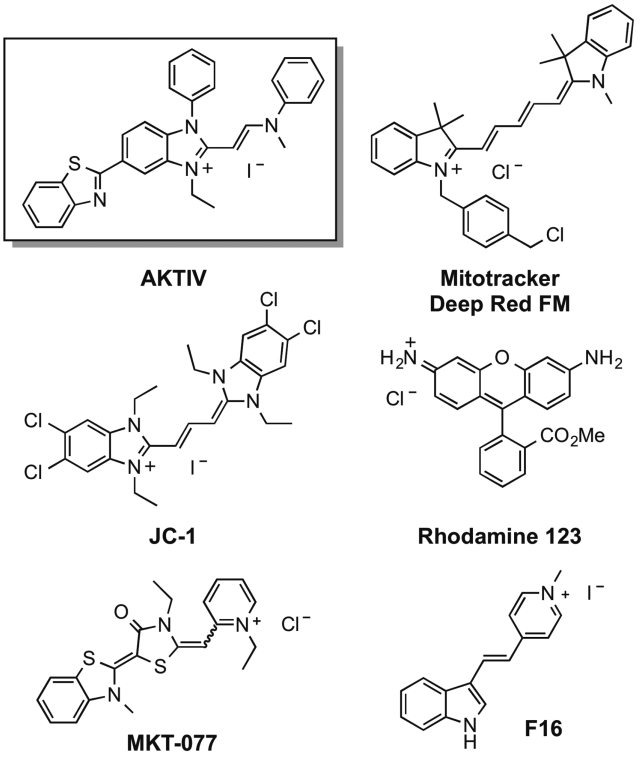

Figure 4. Comparison of the structure of AKTIV with other small molecules that selectively accumulate in mitochondria of mammalian cells.

007,[24,25] and F16.[26] These types of lipophilic delocalized cations are known to accumulate in mitochondria[27,28] and are driven into this organelle by the high negative electrochemical potential that exists across the inner mitochondrial membrane (typically −120 to −180 mV, depending on cell type).[29−32] This negative membrane potential is critical for production of ATP by the mitochondrial F_0F_1-ATP synthase and is generated by pumping of protons across the mitochondrial inner membrane by the respiratory chain.

To quantify the extent of bioaccumulation of small molecules in mitochondria, we initially analyzed the fluorescence of bead standards upon excitation at 405 and 488 nm. This allowed standard curves of molecular equivalents of the fluorophores Cascade Blue (for AKTIV) and fluorescein (for rhodamine 123) to be constructed. Human Jurkat cells were briefly treated with AKTIV or rhodamine 123 for 15 min, subjected to flow cytometry under the same conditions, and the number of fluorophores per cell was calculated based on the brightness of Cascade Blue (Φ = 0.54, $\varepsilon_{399\ nm}$ = 28 000 M^{-1} cm^{-1})[33] and fluorescein ($\Phi_{pH\ 9}$ = 0.93, $\varepsilon_{490\ nm}$ = 76 900 M^{-1} cm^{-1}).[34] As shown in Figure 5, based on the published[35] average cell volume (663.7 μm^3) and mitochondrial volume (33.4 μm^3) of Jurkat lymphocytes, concentrations of rhodamine 123 and AKTIV in mitochondria were determined. These values were

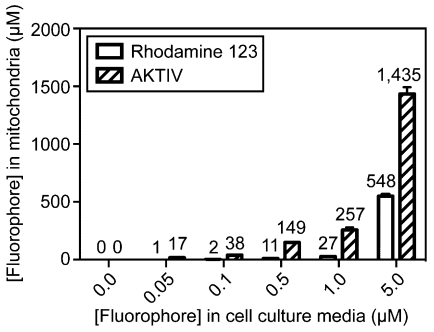

Figure 5. Concentrations of rhodamine 123 (left bars) and AKTIV (right bars) in mitochondria of Jurkat lymphocytes after treatment for 15 min at 37 °C. Treated cells were analyzed by flow cytometry with excitation at 488 nm (rhodamine 123) or 405 nm (AKTIV). Cellular fluorescence was converted to concentration using a standard curve constructed with SpheroTech Rainbow Ultra beads and a ratio of mitochondrial volume to total cell volume of 0.053. These concentrations were corrected to account for quenching of fluorophores observed at high concentrations. Error bars represent the standard deviation.

further corrected to account for the quenching of these fluorophores that occurs at high concentrations (data shown in Figure S1 and methods provided in the Supporting Information). These studies revealed that after treatment of cells with culture media containing 0.05 to 5 μM of these compounds, rhodamine 123 was estimated to reach concentrations of 1−548 μM in mitochondria. Under the same conditions, AKTIV was estimated to accumulate to 17−1435 μM in these organelles. Correspondingly, when 1 μM of AKTIV was added to cells for 15 min, over 250-fold bioaccumulation in mitochondria was observed. This rapid, selective, and massive accumulation in mitochondria provides strong evidence that these organelles are a major and direct target of the biological effects of this small molecule.

To probe the effects of AKTIV on mitochondria, we examined the morphology of these organelles in HeLa cells by confocal laser scanning microscopy. In living cells, mitochondria constantly undergo fusion and fission events, and these dynamic processes play key roles in mitochondrial biogenesis, cellular energetics, apoptosis, and mitochondrial morphology.[36,37] Compared to the vehicle (0.1% DMSO) control, when HeLa cells were treated with AKTIV (1 μM) for 20 min, rapid and extensive swelling of the normally tubular mitochondria was observed (Figure 6). This swelling was followed by similarly rapid disintegration of these organelles into smaller structures (videos showing the time course of these effects are provided in the Supporting Information). As a positive control, hydrogen peroxide was added to induce oxidative stress and disrupt the mitochondrial network.[38] In HeLa cells treated with H_2O_2 (1 mM) for 20−40 min, fragmentation of the mitochondrial network was observed, but this treatment did not cause the swelling or disintegration associated with AKTIV (Figure 6). These results indicate that AKTIV profoundly disrupts the morphology of mitochondria of HeLa cells, inducing distinctive phenotype of swelling followed by disintegration of these organelles.

Elevated mitochondrial membrane potential is a hallmark of cancer.[30,39,40] To examine the effect of AKTIV on cell lines that differ in mitochondrial membrane potential, we compared the toxicity of this compound with an uncharged desethyl analogue (DEAKTIV)[13] toward two cancer cell lines (HeLa and Jurkat)

dx.doi.org/10.1021/cb500856c | ACS Chem. Biol. 2015, 10, 570−576

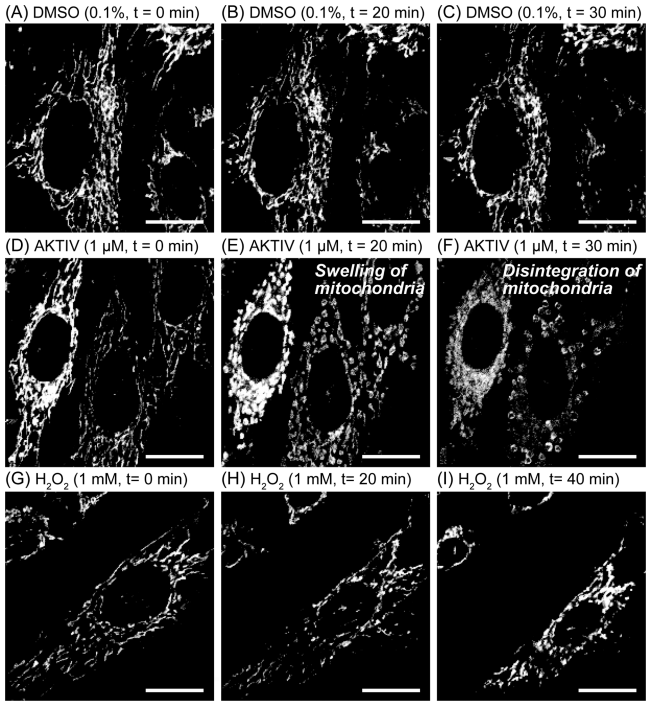

Figure 6. Confocal laser scanning micrographs of living HeLa cells treated with MitoTracker Deep Red FM (100 nM). Cells were further treated with DMSO (0.1%, panels A–C), AKTIV (1 μM, panels D–F), or hydrogen peroxide (1 mM, panels G–I) at 37 °C. The same field of cells was imaged at the three times shown. Scale bar = 20 μm.

and the normal monkey kidney cell line CV-1. The DEAKTIV analogue was chosen as a control because it lacks the fixed positive charge needed to drive accumulation into mitochondria. As shown in Figure 7, AKTIV was highly toxic toward HeLa (IC_{50} = 320 ± 30 nM) and Jurkat (IC_{50} = 340 ± 30 nM)

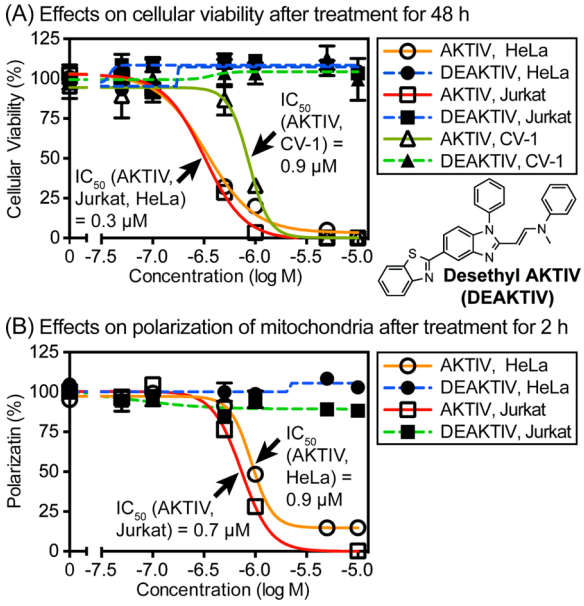

Figure 7. Panel A: Cytotoxicity of AKTIV and the uncharged DEAKTIV analogue toward two cancer cell lines (HeLa, Jurkat) and a normal cell line (CV-1) after 48 h. Panel B: Effects of treatment with these compounds for 2 h on the polarization of mitochondria as assayed with the ratiometric fluorescent probe JC-1 (1 μM).

cells after treatment for 48 h, but under these conditions, this compound was less toxic toward normal CV-1 cells (IC_{50}= 870 ± 90 nM), which have been shown to exhibit a lower inherent mitochondrial membrane potential.[41] The uncharged but structurally similar DEAKTIV analogue was not toxic to any of these cell lines (IC_{50} > 10 μM), providing evidence that the positive charge of AKTIV drives this compound into mitochondria. This interpretation was further supported by confocal imaging of HeLa cells treated with the rapid mitochondrial depolarizer cyanide 3-chlorophenylhydrazine (CCCP, 50 μM, 15 min). This treatment inhibited the uptake of AKTIV by mitochondria, indicating that the negative membrane potential of these organelles is required for accumulation of this compound (confocal microscopy images provided in Figure S2 of the Supporting Information).

To examine the functional consequences of treatment with AKTIV, the fluorescent probe JC-1 (Figure 4) was used to measure effects on the membrane potential of mitochondria. This probe undergoes a shift in fluorescence emission from green to red as it accumulates in mitochondria, and by analysis of this red/green ratio, one can quantify the extent of mitochondrial depolarization. As shown in Figure 7, treatment with AKTIV for 2 h depolarized mitochondria of HeLa cells (IC_{50} = 920 ± 30 nM) and Jurkat cells (IC_{50} = 750 ± 30 nM) at submicromolar concentrations, whereas treatment with DEAKTIV was inconsequential.

Mitochondria predominantly produce cellular ATP during aerobic respiration.[30] To determine whether AKTIV inhibits this process, we used a MitoXpress Xtra-HS assay (Luxcel)[42] to measure the consumption of oxygen by mitochondria in HeLa cells (Figure 8). Consistent with previous studies,[43] CCCP, an uncoupling agent that disrupts mitochondrial electron transport chain activity by bypassing efflux of protons through the ATP synthase complex, accelerated consumption of O_2 compared to vehicle control. In contrast, AKTIV (2 μM) completely blocked consumption of O_2 over the 90 min time course of the experiment. This inhibition was comparable to treatment with 10 μM of the mitochondrial complex I inhibitor rotenone.[43] Addition of LY294002 (10 μM), a well-characterized inhibitor of PI3K/Akt pathway,[44] showed no effect on O_2 consumption, demonstrating that blocking this pathway under these conditions does not affect mitochondrial respiration. This control experiment provides evidence that the inhibition of mitochondrial respiration by AKTIV might be upstream of its effects on the PI3K/Akt pathway.

Reactive oxygen species (ROS) are byproducts of the mitochondrial electron transport chain.[45] High levels of ROS indicate mitochondrial dysfunction and can induce apoptosis.[46] To investigate whether treatment with AKTIV induces changes in cellular ROS, which could link mitochondrial dysfunction to downstream redox-sensitive biological effects such as activation of Akt,[47] we assayed levels of ROS in Jurkat lymphocytes with the fluorescent probe H_2DCFDA. As shown in Figure 8, treatment of Jurkat cells with AKTIV (30 min) increased cellular ROS in a dose-dependent manner by up to 59-fold at 2 μM compared with the vehicle control. Treatment with hydrogen peroxide (30 min) as a positive control increased ROS by 24-fold at 1 μM and 93-fold at 10 μM. Higher concentrations of hydrogen peroxide (50 μM) showed reduced effects that were associated with cytotoxicity. As another control, treatment with rotenone (30 min), an agent previously shown to elevate cellular ROS in HepG2 cells,[48] increased ROS in a dose-dependent manner by up to 16-fold at 50 μM. Given

dx.doi.org/10.1021/cb500856c | ACS Chem. Biol. 2015, 10, 570–576

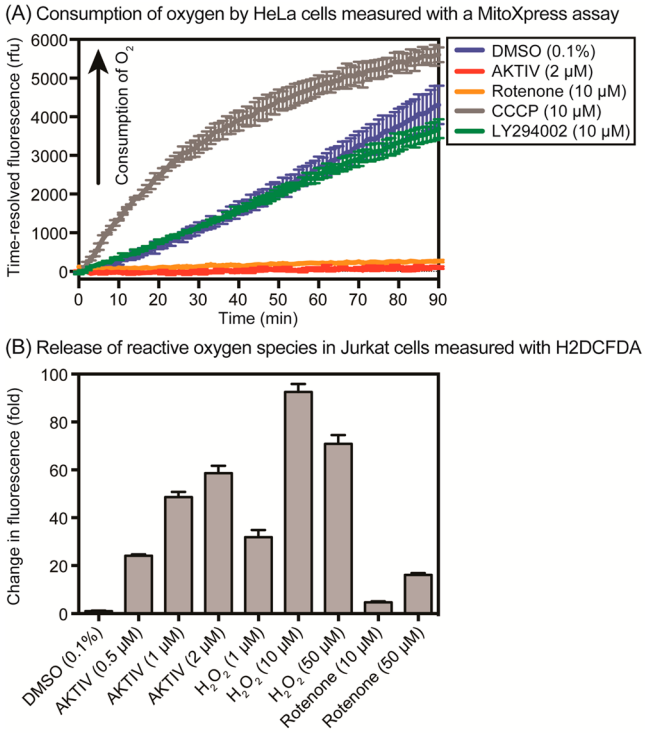

Figure 8. Panel A: Consumption of oxygen by HeLa cells over 90 min as quantified with a MitoXpress XS assay. In negative control experiments with cells treated with DMSO (0.1%) or AKTIV (2 μM) but without addition of the Pt-porphyrin-based MitoXpress probe, no time-resolved fluorescence was observed (data not shown). Panel B: Fluorescence of the ROS sensor H2DCFDA (2 μM) in Jurkat cells. Cells were treated for 30 min followed by analysis by flow cytometry. Error bars represent standard errors of the mean.

that phosphorylation of Akt is redox-sensitive[47] and can be activated by treatment of cells with hydrogen peroxide, these results suggest that the mitochondrial dysfunction and production of ROS by AKTIV may be mechanistically linked to the previously reported[10] activation of Akt.

Conclusions. Based on its effects on the nuclear export of FOXO1a, AKTIV was initially proposed[1] to function as an inhibitor of the PI3K/Akt pathway. However, a more recent investigation by Connor[10] concluded that this compound does not inhibit any known kinases in this signaling pathway; moreover, AKTIV increases phosphorylation of Akt kinase when added to BHK-21 cells at concentrations that elicit major biological effects. To investigate its mechanism of action, we used intrinsic fluorescence to examine the subcellular localization of AKTIV. Imaging of treated HeLa cells by confocal microscopy with excitation at 405 nm revealed mitochondria as a major target of this potent anticancer/antiviral agent. When cancer cell lines were treated with 1 μM of this compound, AKTIV rapidly accumulated to over 250 μM in these organelles within 15 min and caused profound mitochondrial dysfunction. Low concentrations of AKTIV triggered swelling, disintegration, and depolarization of mitochondria, elevation of ROS, and essentially complete inhibition of cellular consumption of oxygen. This rapid elevation of ROS provides a potential mechanistic link between mitochondrial dysfunction induced by AKTIV and increased phosphorylation[10] of the redox-sensitive[47] Akt kinase observed at low concentrations. These studies revealed a novel mechanism of action of AKTIV and provide a new rationale for its anticancer and broad-spectrum antiviral activities.

Due to alterations in glucose metabolism, cancer cells commonly exhibit elevated mitochondrial membrane potentials of at least 60 mV compared with normal cells.[30,39,40] By accumulating in hyperpolarized mitochondria, delocalized lipophilic cations such as rhodamine 123,[23,41] dequinalinium,[49] F16,[26] MKT-077,[24,25] rosamines,[50] and others[27,51,52] can exhibit selective anticancer activity.[53,54] These types of compounds can affect a number of different mitochondrial targets involved in cellular proliferation including mitochondrial polarization,[26] the NADH-ubiquinone reductase,[55] the F_0F_1 ATPase,[27] and pro-apoptotic signals such as Bcl-2 family members.[56] Consequently, the selective anticancer activity of AKTIV can be explained by its profound effects on hyperpolarized mitochondria in the absence of downstream effects on the PI3K/Akt pathway.

Inhibitors of mitochondrial respiration suppress the *de novo* synthesis of pyrimidines.[57] This mechanism of action was recently reported[58] to be responsible for the broad spectrum antiviral activity of the natural product antimycin A, a mitochondrial complex III inhibitor, against RNA viruses. This antiviral activity of antimycin A and analogues was observed at nanomolar concentrations that are not toxic to mammalian host cells. Other compounds similarly shown to exhibit antiviral activity by promoting mitochondrial dysfunction include the complex III inhibitor myxothiazole, the complex I inhibitor rotenone, the proton ionophore CCCP, and the ATP synthase inhibitor oligomycin.[58] Some of these mitochondrial electron transport chain inhibitors exhibit antiviral activity under conditions where ATP production is not suppressed.[58] Based on this precedent, we conclude that the broad spectrum antiviral activity of AKTIV relates to its immediate and direct effects on mitochondria either through suppression of *de novo* synthesis of pyrimidines, the generation of mitochondrial ROS, and/or depletion of cellular ATP. Consequently, identification of mitochondria as a major target of AKTIV, which are profoundly affected within minutes of treatment of mammalian cells at concentrations of ~1−5 μM, provides a unifying explanation for many of the diverse biological activities of this potent small molecule.

■ ASSOCIATED CONTENT

Supporting Information

Experimental methods, concentration-dependent fluorescence quenching data (Figure S1), additional supporting micrographs (Figure S2), and confocal microscopy videos of living HeLa cells showing time-dependent effects of AKTIV on the morphology of mitochondria. Cells shown in the videos were treated with MitoTracker Deep Red FM (100 nM) followed by AKTIV (1 μM) or DMSO (0.1%) for 0−30 min. This material is available free of charge via the Internet at http://pubs.acs.org.

■ AUTHOR INFORMATION

Corresponding Author

*E-mail: brpeters@ku.edu.

Notes

The authors declare no competing financial interest.

■ ACKNOWLEDGMENTS

We thank the National Institutes of Health (NIH; RC1-GM091086, R01-CA83831) and the KU Cancer Center for

financial support. J.M.M. was supported in part by the NIH Dynamic Aspects of Chemical Biology Training Grant at the University of Kansas (T32-GM08545).

REFERENCES

(1) Kau, T. R., Schroeder, F., Ramaswamy, S., Wojciechowski, C. L., Zhao, J. J., Roberts, T. M., Clardy, J., Sellers, W. R., and Silver, P. A. (2003) A chemical genetic screen identifies inhibitors of regulated nuclear export of a Forkhead transcription factor in PTEN-deficient tumor cells. *Cancer Cell 4*, 463−476.

(2) Koeller, K. M., Haggarty, S. J., Perkins, B. D., Leykin, I., Wong, J. C., Kao, M. C., and Schreiber, S. L. (2003) Chemical genetic modifier screens: Small molecule trichostatin suppressors as probes of intracellular histone and tubulin acetylation. *Chem. Biol. 10*, 397−410.

(3) Margalit, D. N., Romberg, L., Mets, R. B., Hebert, A. M., Mitchison, T. J., Kirschner, M. W., and RayChaudhuri, D. (2004) Targeting cell division: Small-molecule inhibitors of FtsZ GTPase perturb cytokinetic ring assembly and induce bacterial lethality. *Proc. Natl. Acad. Sci. U.S.A. 101*, 11821−11826.

(4) Koomoa, D. L., Yco, L. P., Borsics, T., Wallick, C. J., and Bachmann, A. S. (2008) Ornithine decarboxylase inhibition by α-difluoromethylornithine activates opposing signaling pathways via phosphorylation of both Akt/protein kinase B and p27Kip1 in neuroblastoma. *Cancer. Res. 68*, 9825−9831.

(5) Hu, C., Solomon, V. R., Ulibarri, G., and Lee, H. (2008) The efficacy and selectivity of tumor cell killing by Akt inhibitors are substantially increased by chloroquine. *Bioorg. Med. Chem. 16*, 7888−7893.

(6) Conley-LaComb, M. K., Saliganan, A., Kandagatla, P., Chen, Y. Q., Cher, M. L., and Chinni, S. R. (2013) PTEN loss mediated Akt activation promotes prostate tumor growth and metastasis via CXCL12/CXCR4 signaling. *Mol. Cancer 12*, 85.

(7) Takamatsu, R., Takeshima, E., Ishikawa, C., Yamamoto, K., Teruya, H., Heuner, K., Higa, F., Fujita, J., and Mori, N. (2010) Inhibition of Akt/GSK3beta signalling pathway by *Legionella pneumophila* is involved in induction of T-cell apoptosis. *Biochem. J. 427*, 57−67.

(8) Fruman, D. A., and Rommel, C. (2014) PI3K and cancer: Lessons, challenges, and opportunities. *Nat. Rev. Drug Discovery 13*, 140−156.

(9) Garcia-Echeverria, C., and Sellers, W. R. (2008) Drug discovery approaches targeting the PI3K/Akt pathway in cancer. *Oncogene 27*, 5511−5526.

(10) Dunn, E. F., Fearns, R., and Connor, J. H. (2009) Akt inhibitor Akt-IV blocks virus replication through an Akt-independent mechanism. *J. Virol. 83*, 11665−11672.

(11) Blaustein, M., Perez-Munizaga, D., Sanchez, M. A., Urrutia, C., Grande, A., Risso, G., Srebrow, A., Alfaro, J., and Colman-Lerner, A. (2013) Modulation of the Akt pathway reveals a novel link with PERK/eIF2α, which is relevant during hypoxia. *PLoS One 8*, e69668.

(12) Sun, M., Fuentes, S. M., Timani, K., Sun, D., Murphy, C., Lin, Y., August, A., Teng, M. N., and He, B. (2008) Akt plays a critical role in replication of nonsegmented negative-stranded RNA viruses. *J. Virol. 82*, 105−114.

(13) Sun, Q., Wu, R., Cai, S., Lin, Y., Sellers, L., Sakamoto, K., He, B., and Peterson, B. R. (2011) Synthesis and biological evaluation of analogues of AKT (protein kinase B) inhibitor-IV. *J. Med. Chem. 54*, 1126−1139.

(14) Luthra, P., Sun, D., Wolfgang, M., and He, B. (2008) AKT1-dependent activation of NF-κB by the L protein of parainfluenza virus 5. *J. Virol. 82*, 10887−10895.

(15) Lavis, L. D., and Raines, R. T. (2014) Bright building blocks for chemical biology. *ACS Chem. Biol. 9*, 855−866.

(16) Lavis, L. D., and Raines, R. T. (2008) Bright ideas for chemical biology. *ACS Chem. Biol. 3*, 142−155.

(17) Loving, G. S., Sainlos, M., and Imperiali, B. (2010) Monitoring protein interactions and dynamics with solvatochromic fluorophores. *Trends Biotechnol. 28*, 73−83.

(18) Williams, A. T., and Winfield, S. A. (1983) Relative fluorescence quantum yields using a computer-controlled luminescence spectrometer. *Analyst 108*, 1067−1071.

(19) Sun, W. C., Gee, K. R., and Haugland, R. P. (1998) Synthesis of novel fluorinated coumarins: Excellent UV-light excitable fluorescent dyes. *Bioorg. Med. Chem. Lett. 8*, 3107−3110.

(20) Rodrigues, R. M., Macko, P., Palosaari, T., and Whelan, M. P. (2011) Autofluorescence microscopy: A non-destructive tool to monitor mitochondrial toxicity. *Toxicol. Lett. 206*, 281−288.

(21) Shim, S. H., Xia, C., Zhong, G., Babcock, H. P., Vaughan, J. C., Huang, B., Wang, X., Xu, C., Bi, G. Q., and Zhuang, X. (2012) Super-resolution fluorescence imaging of organelles in live cells with photoswitchable membrane probes. *Proc. Natl. Acad. Sci. U.S.A. 109*, 13978−13983.

(22) Liu, T., Hannafon, B., Gill, L., Kelly, W., and Benbrook, D. (2007) Flex-Hets differentially induce apoptosis in cancer over normal cells by directly targeting mitochondria. *Mol. Cancer Ther. 6*, 1814−1822.

(23) Modica-Napolitano, J. S., and Aprille, J. R. (1987) Basis for the selective cytotoxicity of rhodamine 123. *Cancer Res. 47*, 4361−4365.

(24) Modica-Napolitano, J. S., Koya, K., Weisberg, E., Brunelli, B. T., Li, Y., and Chen, L. B. (1996) Selective damage to carcinoma mitochondria by the rhodacyanine MKT-077. *Cancer Res. 56*, 544−550.

(25) Wadhwa, R., Sugihara, T., Yoshida, A., Nomura, H., Reddel, R. R., Simpson, R., Maruta, H., and Kaul, S. C. (2000) Selective toxicity of MKT-077 to cancer cells is mediated by its binding to the hsp70 family protein mot-2 and reactivation of p53 function. *Cancer Res. 60*, 6818−6821.

(26) Fantin, V. R., Berardi, M. J., Scorrano, L., Korsmeyer, S. J., and Leder, P. (2002) A novel mitochondriotoxic small molecule that selectively inhibits tumor cell growth. *Cancer cell 2*, 29−42.

(27) Modica-Napolitano, J. S., and Aprille, J. R. (2001) Delocalized lipophilic cations selectively target the mitochondria of carcinoma cells. *Adv. Drug Delivery Rev. 49*, 63−70.

(28) Rin Jean, S., Tulumello, D. V., Wisnovsky, S. P., Lei, E. K., Pereira, M. P., and Kelley, S. O. (2014) Molecular vehicles for mitochondrial chemical biology and drug delivery. *ACS Chem. Biol. 9*, 323−333.

(29) Nicholls, D. G. (1974) The influence of respiration and ATP hydrolysis on the proton-electrochemical gradient across the inner membrane of rat-liver mitochondria as determined by ion distribution. *Eur. J. Biochem. 50*, 305−315.

(30) Chen, L. B. (1988) Mitochondrial membrane potential in living cells. *Annu. Rev. Cell Biol. 4*, 155−181.

(31) Perry, S. W., Norman, J. P., Barbieri, J., Brown, E. B., and Gelbard, H. A. (2011) Mitochondrial membrane potential probes and the proton gradient: A practical usage guide. *Biotechniques 50*, 98−115.

(32) Belostotsky, I., da Silva, S. M., Paez, M. G., and Indig, G. L. (2011) Mitochondrial targeting for photochemotherapy. Can selective tumor cell killing be predicted based on *n*-octanol/water distribution coefficients? *Biotechnic. Histochem. 86*, 302−314.

(33) Whitaker, J. E., Haugland, R. P., Moore, P. L., Hewitt, P. C., Reese, M., and Haugland, R. P. (1991) Cascade Blue derivatives: Water soluble, reactive, blue emission dyes evaluated as fluorescent labels and tracers. *Anal. Biochem. 198*, 119−130.

(34) Sjoback, R., Nygren, J., and Kubista, M. (1995) Absorption and Fluorescence Properties of Fluorescein. *Spectrochim. Acta, Part A 51*, L7−L21.

(35) Feng, Y., Zhang, N., Jacobs, K. M., Jiang, W., Yang, L. V., Li, Z., Zhang, J., Lu, J. Q., and Hu, X.-H. (2014) Polarization imaging and classification of Jurkat T and Ramos B cells using a flow cytometer. *Cytometry Part A 85*, 817−826.

(36) Westermann, B. (2010) Mitochondrial fusion and fission in cell life and death. *Nat. Rev. Mol. Cell Biol. 11*, 872−884.

(37) Karbowski, M., and Youle, R. J. (2003) Dynamics of mitochondrial morphology in healthy cells and during apoptosis. *Cell Death Differ. 10*, 870−880.

(38) Fan, X., Hussien, R., and Brooks, G. A. (2010) H_2O_2-induced mitochondrial fragmentation in C2C12 myocytes. *Free Radical Biol. Med. 49*, 1646−1654.
(39) Kadenbach, B. (2003) Intrinsic and extrinsic uncoupling of oxidative phosphorylation. *Biochim. Biophys. Acta 1604*, 77−94.
(40) Wallace, D. C. (2012) Mitochondria and cancer. *Nat. Rev. Cancer 12*, 685−698.
(41) Lampidis, T. J., Bernal, S. D., Summerhayes, I. C., and Chen, L. B. (1983) Selective toxicity of rhodamine 123 in carcinoma cells *in vitro*. *Cancer Res. 43*, 716−720.
(42) O'Riordan, T. C., Zhdanov, A. V., Ponomarev, G. V., and Papkovsky, D. B. (2007) Analysis of intracellular oxygen and metabolic responses of mammalian cells by time-resolved fluorometry. *Anal. Chem. 79*, 9414−9419.
(43) Marroquin, L. D., Hynes, J., Dykens, J. A., Jamieson, J. D., and Will, Y. (2007) Circumventing the crabtree effect: Replacing media glucose with galactose increases susceptibility of HepG2 cells to mitochondrial toxicants. *Toxicol. Sci. 97*, 539−547.
(44) Vlahos, C. J., Matter, W. F., Hui, K. Y., and Brown, R. F. (1994) A specific inhibitor of phosphatidylinositol 3-kinase, 2-(4-morpholinyl)-8-phenyl-4H-1-benzopyran-4-one (LY294002). *J. Biol. Chem. 269*, 5241−5248.
(45) Sena, L. A., and Chandel, N. S. (2012) Physiological roles of mitochondrial reactive oxygen species. *Molecular cell 48*, 158−167.
(46) Fleury, C., Mignotte, B., and Vayssière, J.-L. (2002) Mitochondrial reactive oxygen species in cell death signaling. *Biochimie 84*, 131−141.
(47) Ushio-Fukai, M., Alexander, R. W., Akers, M., Yin, Q., Fujio, Y., Walsh, K., and Griendling, K. K. (1999) Reactive oxygen species mediate the activation of Akt/protein kinase B by angiotensin II in vascular smooth muscle cells. *J. Biol. Chem. 274*, 22699−22704.
(48) Siddiqui, M. A., Ahmad, J., Farshori, N. N., Saquib, Q., Jahan, S., Kashyap, M. P., Ahamed, M., Musarrat, J., and Al-Khedhairy, A. A. (2013) Rotenone-induced oxidative stress and apoptosis in human liver HepG2 cells. *Mol. Cell. Biochem. 384*, 59−69.
(49) Weiss, M. J., Wong, J. R., Ha, C. S., Bleday, R., Salem, R. R., Steele, G. D., Jr., and Chen, L. B. (1987) Dequalinium, a topical antimicrobial agent, displays anticarcinoma activity based on selective mitochondrial accumulation. *Proc. Natl. Acad. Sci. U.S.A. 84*, 5444−5448.
(50) Lim, S. H., Wu, L., Burgess, K., and Lee, H. B. (2009) New cytotoxic rosamine derivatives selectively accumulate in the mitochondria of cancer cells. *Anticancer Drugs 20*, 461−468.
(51) Fonseca, S. B., Pereira, M. P., Mourtada, R., Gronda, M., Horton, K. L., Hurren, R., Minden, M. D., Schimmer, A. D., and Kelley, S. O. (2011) Rerouting chlorambucil to mitochondria combats drug deactivation and resistance in cancer cells. *Chem. Biol. 18*, 445−453.
(52) Horton, K. L., Stewart, K. M., Fonseca, S. B., Guo, Q., and Kelley, S. O. (2008) Mitochondria-penetrating peptides. *Chem. Biol. 15*, 375−382.
(53) Smith, R. A., Hartley, R. C., and Murphy, M. P. (2011) Mitochondria-targeted small molecule therapeutics and probes. *Antioxid. Redox Sign. 15*, 3021−3038.
(54) Wang, F., Ogasawara, M. A., and Huang, P. (2010) Small mitochondria-targeting molecules as anti-cancer agents. *Mol. Asp. Med. 31*, 75−92.
(55) Anderson, W. M., Patheja, H. S., Delinck, D. L., Baldwin, W. W., Smiley, S. T., and Chen, L. B. (1989) Inhibition of bovine heart mitochondrial and *Paracoccus denitrificans* NADH—Ubiquinone reductase by dequalinium chloride and three structurally related quinolinium compounds. *Biochem Int. 19*, 673−685.
(56) Fantin, V. R., and Leder, P. (2006) Mitochondriotoxic compounds for cancer therapy. *Oncogene 25*, 4787−4797.
(57) Loffler, M., Jockel, J., Schuster, G., and Becker, C. (1997) Dihydroorotate-ubiquinone oxidoreductase links mitochondria in the biosynthesis of pyrimidine nucleotides. *Mol. Cell. Biochem. 174*, 125−129.
(58) Raveh, A., Delekta, P. C., Dobry, C. J., Peng, W., Schultz, P. J., Blakely, P. K., Tai, A. W., Matainaho, T., Irani, D. N., Sherman, D. H., and Miller, D. J. (2013) Discovery of potent broad spectrum antivirals derived from marine actinobacteria. *PLoS One 8*, e82318.